PROCEEDINGS OF ECOS 2018 – THE 31ST INTERNATIONAL CONFERENCE ON
EFFICIENCY, COST, OPTIMIZATION, SIMULATION AND ENVIRONMENTAL IMPACT OF ENERGY SYSTEMS
JUNE 17-22, 2018, GUIMARÃES, PORTUGAL

An analysis of the retrofitting potential of a subcritical ORC into a partial evaporating ORC under off-design operation

Steven Lecompte[a], Michel de Paepe[a]

[a] Department of Flow, Heat, and Combustion Mechanics, Ghent University - UGent, Sint-Pietersnieuwstraat 41, 9000 Gent, Belgium, CA:steven.lecompte@ugent.be, michel.depaepe@ugent.be

Abstract:
Many applications where ORCs are installed have time varying waste heat streams. To account for this, flexible and robust off-design models are necessary. In addition, alternative operating conditions and cycle architectures show potential for increased performance. This work investigates how operation as a partial evaporating cycle (PEORC) affects the performance of the ORC. More specifically, the question is raised if current subcritical ORC (SCORC) installations provide potential to be retrofitted into PEORC operation by analysing their off-design operation. The initial results show that under these conditions the PEORC shows a potential net power output increase between 2% to 12% relative to the base SCORC depending on the off-design conditions. The optimal expander inlet vapour fraction that maximises the net power output ranges between 0.5 and 1. With roughly the same maximum pressures, the same working fluid, and an adapted measuring and control strategy, significant net power improvements could thus be achieved. It is important to note that for PEORC operation the performance of the pump becomes determinative. Installing a pump with a better efficiency would further benefit operation as PEORC. Based on these results, there are clearly opportunities in retrofitting existing SCORC systems.

Keywords:
Organic Rankine cycle, Triangular cycle, Thermodynamics, Wet-expansion.

1. Introduction

The organic Rankine cycle (ORC) is a mature technology for low temperature energy conversion. However before large scale adoption is considered, companies need to be convinced of the benefits. Considering the appraisal of an ORC project is mainly motivated by the financial gain, an accurate prediction of the power output is essential. Yet, many of the applications where ORCs are deployed have time varying energy streams. Examples of these are capacity and temperature variations in process streams which can amongst others be found in the cement industry (drying processes) [1], transportation sector (mobile combustion engines) [2] and steel industry (electric arc furnaces, cokes ovens) [3, 4]. These variations add complexity to the assessment of the real power output of the organic Rankine cycle. As such, detailed models are necessary to account for off-design or part-load operation.

In the research literature there is a specific focus on the part-load and off-design operation of the basic subcritical ORC. Gurgenci [5] analysed the part-load performance of ORCs for solar applications. Sun and Li [6] investigated the part load performance of ORCs for waste heat valorisation. Manente et al. [7] simulated the part load performance of a geothermal plant. Ibarra et al. [8] simulated a 5 kWe ORC at part-load operation. Hu et al. [9] investigated the off-design performance under different control strategies.

To further increase the adoption rate for low-temperature ORCs (<150 °C), an increase in conversion efficiency would be most valuable. Alternative ORC architectures are known to provide increased power output from the same waste heat stream [10]. For waste heat recovery applications the partial evaporation ORC (PEORC) shows great potential [10, 11]. In a PEORC the working fluid is not superheated, but exits the evaporator as a two-phase flow. This results in increased mass flow rate of the ORC working fluid due to omitting the enthalpy of vaporization. Furthermore, an adapted control algorithm is required as normally the set-point of the control system is based on the level of superheat after the evaporator. Typically, a black box cycle analysis is employed to assess

the performance benefit of new architectures/working fluids; this black-box approach is advantageous because of its calculation speed. The optimisation objective and optimisation parameters are directly derived from the first and the second law of thermodynamics. A broad selection of working fluids [12–17] and cycle architectures [11, 18-23], can be investigated in an acceptable time-frame. However the actual component behaviour and thus also off-design or part-load operation is completely neglected.

In this work, the off-design performance of a subcritical ORC (SCORC) and a partial evaporating ORC (PEORC) is investigated. Detailed off-design component models from a previous work by the authors were used. These models were calibrated and validated on a small scale subcritical ORC. The extension to operate as a PEORC has been done by adapting the expander model equations. More specifically, the question is raised if current SCORC installations provide potential to be retrofitted into PEORC operation.

2. ORC layout and modelling method

2.1. ORC component models

The modelling choices and equations are detailed in the PhD of Lecompte [24]. In the cited work, an extensive discussion on the solution strategy is provided. In this section, the modelling scheme is only shortly introduced. The implemented model of the heat exchanger is a hybrid approach between the finite volume models [25] and the moving boundary models [26]. The main benefit of the moving boundary model is the fast calculation time, while the finite volume models show increased accuracy for complex geometries and for fluids with thermophysical properties which cannot be assumed constant during heating while omitting phase transitions. Finite volume models however are at the expense of an increased computational time. Initially, the heat exchanger is discretised in N=58 segments. These segments are interconnected according to the geometry of the heat exchangers. The P-NTU [27] correlations are used to determine the heat transfer in each segment. If there is a phase transition, an additional segment is inserted. The lengths of the transition segments are calculated and the solver continues with calculating the heat transfer for the next segment. The calculation stops if all segments are handled. If N=0 the model is equal to a moving boundary model. The convective heat transfer correlations for plate heat exchanger are taken from: Martin [28] (single-phase), Han et al. [29] (two-phase evaporation) and Han et al. [30] (two-phase condensation). The semi-empirical expander model is characterized by three main equations. Eq. 3, as given by Declaye et al. [31], models the filling factor.

$$r_p^* = \frac{r_p - 4}{4}, \tag{1}$$

$$p^* = \frac{p_{exp,in} - 10}{10}, \tag{2}$$

$$\psi = a_1 + a_2 ln\left(\frac{N_{exp}}{5000}\right) + a_3 r_p^* + a_4 p^*, \tag{3}$$

The filling factor directly specifies the mass flow rate trough the expander by use of Eq. 4. The internal built in volume, $V_{exp,internal}$, is taken as 66.15 cm³.

$$\psi = \frac{\dot{m}_{wf} v_{exp,in}}{V_{exp,internal} N_{exp}}, \tag{4}$$

The remaining two equations model the electrical power output and the internal enthalpy drop, they are respectively Eq. 5 and Eq. 6. This formulation is inspired by the model of Lemort et al. [32]. The complete expander model thus requires 8 coefficients ($a_1, a_2, a_3, a_4, \eta_{loss,exp,cycle}, \eta_{loss,exp,grid}, r_{v,exp,cycle}, r_{v,exp,grid}$) that need calibration.

$$\dot{W}_{exp,cycle} = \eta_{loss,exp,cycle}\dot{m}_{wf}\left[\left(h_{exp,in} - h_{exp,internal}\right) + \left(p_{exp,internal} - p_{exp,out}\right)v_{internal}r_{v,exp,cycle}\right], \quad (5)$$

$$\dot{W}_{exp,grid} = \eta_{loss,exp,grid}\dot{m}_{wf}\left[\left(h_{exp,in} - h_{exp,internal}\right) + \left(p_{exp,internal} - p_{exp,out}\right)v_{internal}r_{v,exp,grid}\right], \quad (6)$$

Volumetric expanders are considered suitable for two-phase expansion, yet limited experimental results are presented [33]. For example, Smith et al. [34], performed measurements on double screw expanders with inlet vapour qualities from 50% to 25%. They showed isentropic efficiencies ranging between 40% and 80%. Li et al. [35] studied a rolling piston-type two-phase expander reporting isentropic efficiencies of 58.7%. A trend, indicating reduced isentropic efficiencies under two-phase expansion for high efficiency single phase double screw machines and vice versa, was shown by Öhman and Lundqvist [33]. They proposed a simplified model [36]; see Eq. 7 and Eq. 8, which relates the isentropic efficiency of superheated or saturated inlet conditions to the isentropic efficiency for two-phase inlet. The cut-off point is found at $\epsilon_{single-phase,peak}$ = 60%. For lower values of $\epsilon_{single-phase,peak}$ the isentropic efficiency for two-phase inlet is increased over the isentropic efficiency under single phase inlet. They explain this due to a decrease in leakage because of the sealing of leakage paths by the liquid phase. However, they state that the available test data in literature is scarce and that the actual behaviour of the two-phase expansion is unknown. In this work, the peak isentropic efficiency of the expander is around 60% so we prefer to analyse the worst case scenario without taking into account the possibly improved performance.

$$\epsilon_{two-phase} = \epsilon_{single-phase,sat} + \psi_{two-phase}(1 - x_{in})/10, \quad (7)$$

$$\psi_{two-phase} = -0.15\epsilon_{single-phase,peak} + 0.09, \quad (8)$$

The centrifugal pump is modelled based on information given by the manufacturer. The characteristic curves of the pump are in function of three dimensionless variables; $C_{\dot{V}}$ (Eq. 9) C_H (Eq. 10) and $\epsilon_{pump,grid}$ (Eq. 11). The characteristic curve depicts the results of a single stage. The reported curve corresponds with low specific speed centrifugal pumps [37, 38]. The optimal operating points for this centrifugal pump would be around $C_{\dot{V}}$ = 0.007. Most of the operating points center around the point $C_{\dot{V}}$ = 0.0057.

$$C_{\dot{V}} = \frac{\dot{V}}{ND^3}, \quad (9)$$

$$C_H = \frac{gH}{N^2D^2}, \quad (10)$$

$$\epsilon_{pump,grid} = \frac{\rho\dot{V}_{pump}gH}{\dot{W}_{pump,grid}}, \quad (11)$$

In general, the models developed proved to be very robust while having a low computational time. The heat exchanger model is computationally the most intensive and takes less than 3.5 seconds in order to solve 11 data points on a single Intel Xeon E5-2640 v3 core.

2.2. Calibration and validation

The proposed models are all semi-empirical and thus calibration on experimental data is required. An 11 kWe organic Rankine cycle set-up was used to perform experimental measurements to characterize the off-design performance. The experimental set-up is a scaled-down version of a real commercial ORC system designed for low heat-source temperatures (between 80 °C and 150 °C) and uses R245fa as the working fluid. The same set-up was also used for characterizing the performance of a single-screw expander [39]. The current set-up includes a double screw expander, centrifugal pump and plate heat exchangers for the evaporator and condenser. The calibration and

subsequent validation is extensively described in the PhD of Lecompte [24]. Details about the experimental setup, the geometry, the nominal operating values and the data reduction techniques can be found there but are omitted in this work for conciseness. The sampling plan includes heat source mass flow rates in the range of 1.5 kg/s to 3 kg/s, cold water volumetric flow rates in the range of 7 m³/h to 14.5 m³/h and heat source temperature levels in the range of 110 °C to 120 °C. In this section, the main conclusions of that paper are only shortly summarized.

The expander is the essentially the only custom made component that necessitates calibration. For the pump, the datasheet of the manufacturer is used, while for the heat exchangers, well known heat transfer and pressure drop correlations are available. The obtained calibration coefficients for the expander can be found in Table 1. The validation results show a closed heat balance of evaporator and condenser with a maximum deviation between secondary and primary heat flow rate of ±5%. Note that the condenser pressure will vary according to the load. The only input parameters to the cycle model are pump and expander rotational speeds. The important dependent parameters are the evaporation pressure, the condensation pressure and the working fluid mass flow rate. All three predicted parameters show a maximum deviation of less than ±1% from the measured value. The modelled net power output deviates less than ±2% from the measured value. In general, this is a satisfactory result that gives confidence in using these models in further analysis.

Table 1. Model calibration coefficients for the expander.

a_1	a_2	a_3	a_4	$\eta_{loss,exp,cycle}$	$\eta_{loss,exp,grid}$	$r_{v,exp,cycle}$	$r_{v,exp,grid}$
1.0632	0	0.0438	0	0.6131	0.5148	4.4953	5.5764

3. Off-design operation and optimization

The validated models are now used to examine the optimal control set points of the experimental set-up. The control variables are the pump and the expander speed. As with most commercial ORC installations, the generator is assumed to be directly connected to the grid, so that the expander rotates at fixed speed. In this work, the expander speed is fixed at 5000 rpm. Changes in the condensing pressure can be imposed by changing the volumetric flow rate of the cooling loop. Similar input boundary conditions as those from the experimental validation campaign are used in this section. The cooling water inlet temperature is assumed fixed at 30 °C.

3.1. Effect of the pump rotational speed

To analyse the optimisation potential, the effect of the pump speed on the cycle operation is investigated. The typical trend of the expander inlet vapour quality, the pump inlet power, the expander outlet power and the net power output in function the pump speed is shown in Fig. 1. The expander output power rises sharply until approximately $x_{exp,in}$ = 0.5 and keeps steadily increasing after this point. For the net power output there is a steady increase until the point of saturated vapour. After this point the pumping power has a detrimental impact on the net power output. The maximum net power output is seen at $x_{exp,in}$ = 0.587 but the sensitivity on the pumping speed is low in this region. Thus slightly lower values of N_{pump} corresponding with higher $x_{exp,in}$ are more interesting. Less working fluid mass flow rate circulates and the pumping power is lower while the effect on the net power output is negligible. Furthermore, as expected from the model by Öhman and Lundqvist [36], the effect of a decreased vapour quality on the expander isentropic efficiency is low. A maximum relative decrease of 2% in adiabatic expander efficiency is seen for a pump speed of 2500 RPM ($x_{exp,in}$ = 0.36). Lower vapour qualities are in practice not achievable as the pump under consideration does not allow for higher rotational speeds.

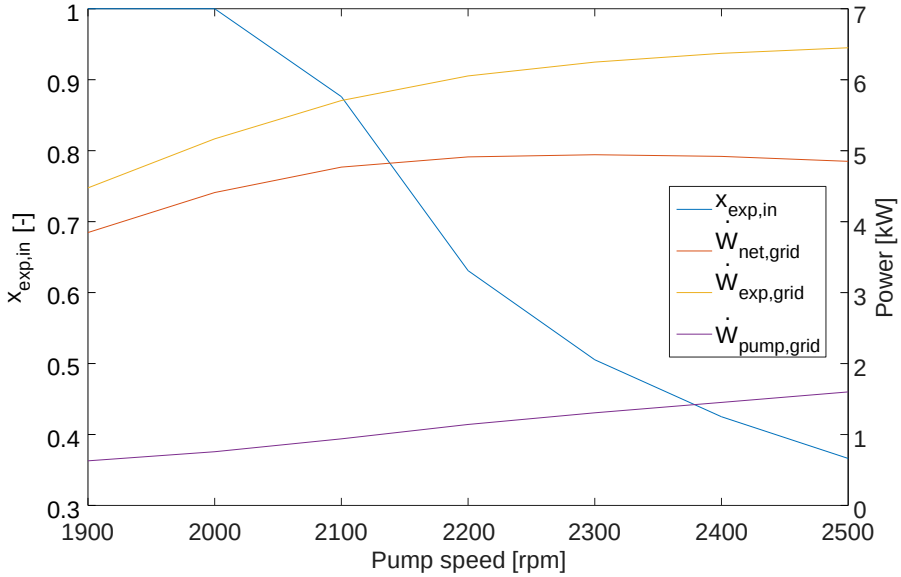

Fig. 1. Cycle parameters $x_{exp,in}$,$\dot{W}_{net}$,$\dot{W}_{net,grid}$,$\dot{W}_{pump,grid}$ in function of N_{pump} for $\dot{m}_{hf}$=1.5kg/s, $T_{hf,in}$=110 °C and $\dot{V}_{cf}$=13.4 m³/h.

3.2. Optimised pump rotational speed

The optimal pump speed, that maximises the net power output, is determined for the list of boundary conditions in Table 2. This list comprises the typical working region of the system. The optimal pump speed and expander inlet vapour quality that corresponds with maximum $\dot{W}_{net}$ is added to Table 2.

Table 2. Range of ORC boundary conditions, results of the optimisation of the pump speed with no constraints on superheating.

$\dot{m}_{hf}$ (kg/s)	T_{hf} (°C)	$\dot{V}_{cf}$ (m³/h)	$N_{pump,opt}$ (RPM)	$\dot{m}_{wf}$ (kg/s)	$x_{exp,in}$ (-)	$p_{exp,in}$ (bar)	$\dot{W}_{net}$ (kW)
1.5	110	7	2198	0.557	0.587	9.92	4.25
1.5	110	13.4	2295	0.630	0.509	9.83	4.94
1.5	120	7	2394	0.527	0.759	11.74	5.44
1.5	120	13.4	2456	0.617	0.634	11.63	6.25
3	110	7	2374	0.558	0.711	11.71	5.43
3	110	13.4	2536	0.700	0.551	11.61	6.28
3	120	7	2542	0.502	0.980	14.02	6.95
3	120	13.4	2603	0.541	0.916	13.97	7.84

The first thing to notice is that the optimised system always works as a PEORC. Yet, the vapour fraction at the inlet of the expander is high compared with previous theoretical results from Lecompte et al. [11]. In the cited work, the conclusion was that a pure triangular cycle (TLC), with vapour quality equal to zero, is thermodynamically the best for maximum net power generation. The explanation for this different behaviour is found in the increasing mass flow rate when omitting the enthalpy of vaporisation. With a low isentropic efficiency of the pump, the required pumping power rises faster than the increase in expander power, see also Fig. 1. The isentropic efficiency of the pump in the set-up is around 20%, this is a lot lower than the 70% from the theoretical assessment [11]. This low value of pump isentropic efficiency is however in line with other experimental results found in literature [40]. When artificially increasing the isentropic efficiency, the optimised cycle again shifts to lower vapour fractions as expected. Thus, when designing the PEORC, the importance of a high efficiency pump should be stressed.

Secondly, for increased hot fluid mass flow rates and temperatures, the optimal pump speed will shift to higher values. The increased pump speed is associated with an increased pumping power and will again lead to an increase in the optimal $x_{exp,in}$ as explained before. The pressure in the system is comprised between 9.9 bar and 14 bar, with the higher values corresponding to higher waste heat input and lower cooling mass flow rates. Notice also that while the PEORC operation is simulated based on the detailed semi-empirical models, further validation in this operating regime is still necessary.

3.3. Comparison between the SCORC and PEORC

Next, the ORC is optimised under the additional constraint of fixed superheating. The level of superheat is commonly used as setpoint to control the SCORC. To make sure that under transient conditions a minimum superheat is attained, the setpoint is set to a safe value. During the experiments a value of 15 °C was the minimum superheat temperature under which robust control was achieved. This value is now imposed as additional constraint and the same optimisation was performed as in the previous section. The results are shown in Table 3.

Table 3. Range of ORC boundary conditions, results of the optimisation of the pump speed with superheat constraint to 15°C.

$\dot{m}_{hf}$ (kg/s)	T_{hf} (°C)	$\dot{V}_{cf}$ (m³/h)	$N_{pump,opt}$ (RPM)	$\dot{m}_{wf}$ (kg/s)	$p_{exp,in}$ (bar)	$\dot{W}_{net}$ (kW)
1.5	110	7	2003	0.308	9.84	4.07
1.5	110	13.4	2029	0.309	9.83	4.55
1.5	120	7	2228	0.367	11.61	5.34
1.5	120	13.4	2255	0.368	11.59	5.93
3	110	7	2172	0.352	11.15	5.02
3	110	13.4	2199	0.353	11.14	5.59
3	120	7	2458	0.435	13.54	6.69
3	120	13.4	2483	0.433	13.47	7.39

Compared to the operation as a PEORC, the optimal rotational speed is around 200 rpm lower. This leads to working fluid mass flow rates which are roughly half of that of the PEORC. The evaporation pressure in the SCORC system is slightly lower, in the order of a few 10 kPa. The relative increase in net power output for a PEORC compared to the SCORC is given in Fig. 2. The relative net power improvements range between 2% and 12%.

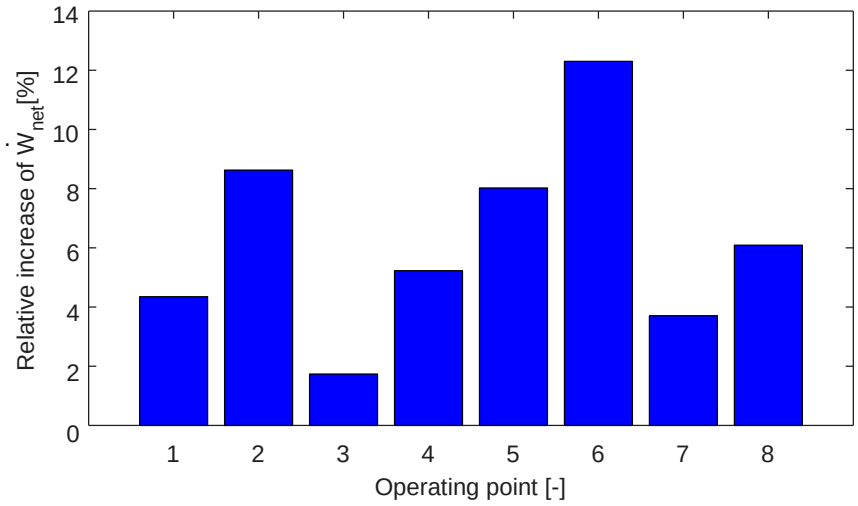

Fig. 2. Relative improvement in $\dot{W}_{net}$ for PEORC operation compared to SCORC, operating points from left to right correspond with the operating points in Table 2 from top to bottom.

As already mentioned, the isentropic efficiency of the pump has a decisive impact on the achievable performance of the PEORC. Let us therefore assume a pump with thrice the isentropic efficiency of the set-up. Thus the isentropic efficiency goes up from approximately 20% to 60%. Under these conditions, the optimal mass flow rate in the PEORC is further increased leading to lower $x_{exp,in}$. In this case performance benefits up to 40% are attainable. Thus, as the pump isentropic efficiency increases, the optimal cycle architecture transitions from SCORC to TLC through PEORC in a continuous manner.

Based on these results, there are clearly opportunities in retrofitting existing SCORC systems. With roughly the same maximum pressures, the same working fluid, and an adapted measuring and control strategy, significant net power improvements can be achieved. However the importance of the pump in a PEORC system should not be stressed.

4. Conclusions

Off-design ORC models were used to optimise the pump rotational speed under different operational regimes. For increased pump rotational speed, the operational regime gradually changes from operation as a subcritical ORC (SCORC) to operation as a partial evaporating ORC (PEORC). During this process the expander power increases steadily. However, looking at the net power output, the high pumping power counteracts this effect. The high pumping power is partially due to the low isentropic efficiency (around 20%) of the pump in the set-up. The optimal expander inlet vapour fraction ($x_{exp,in}$) that maximises the net power output, ranges between 0.5 and 1. This is in contrast to theoretical studies [11], which show that the ideal operating point with a good performing pump (isentropic efficiency 70%) and an optimised fluid selection, is a triangular cycle (TLC) ($x_{exp,in}$ = 0). Comparing the operation as SCORC and PEORC, the PEORC shows an increased net power output between 2% to 12% over the SCORC. When the pump isentropic efficiency is tripled, the PEORC can show performance increases up to 40%. As the pump isentropic efficiency increases, the optimal cycle architecture transitions from SCORC to TLC through PEORC in a continuous manner. To achieve optimal operating conditions under increased loads, it is furthermore advisable to increase the expander rotational speed.

Acknowledgments

The results presented in this paper were obtained within the frame of the IWT SBO- 110006 project The Next Generation organic Rankine cycles (www.orcnext.be), funded by the Institute for the Promotion and Innovation by Science and Technology in Flanders. This financial support is gratefully acknowledged. Steven Lecompte is a postdoctoral fellow of the Research Foundation-Flanders (FWO, 12T6818N). Data supporting this publication can be obtained on request from steven.lecompte@ugent.be.

Nomenclature

A area, m²

C_H dimensionless mass flow rate, -

$C_{\dot{V}}$ dimensionless volume flow rate, -

D diameter, m

g standard gravity, m/s²

H head, m

h specific enthalpy, J/kg

$\dot{m}$ mass flow rate, kg/s

N rotational speed

P temperature effectiveness, -

p pressure, Pa

$\dot{Q}$ heat transfer rate, W

R heat capacity ratio, -

r_p pressure ratio, -

r_v built-in volume ratio, -

T temperature, °C

$\dot{V}$ volumetric flow rate, m³/s

$V_{exp,internal}$ built-in volume, m³

$\dot{W}$ power, W

x vapour fraction, -

Abbreviations

LMTD log-mean temperature difference

NTU number of transfer units

ORC organic Rankine cycle

PEOR partial evaporating organic Rankine cycle

SCORC subcritical organic Rankine cycle

Greek symbols

ϵ isentropic efficiency, -

η loss factor, -

ψ filling factor, -

ρ density, kg/m³

Subscripts and superscripts

cf cold fluid

cond condenser

el electrical

evap evaporator

exp expander

grid electrical grid

hf hot fluid

in inlet

out outlet

wf working fluid

References

[1] Legmann H., Recovery of industrial heat in the cement industry by means of the ORC process. IEEE-IAS/PCA 44th Cement Industry Technical Conference; 2002 ; Jacksonville, Florida, USA; IEEE: 29–35.

[2] Horst T.A., Rottengruber H., Seifert M., Ringler J., Dynamic heat exchanger model for performance prediction and control system design of automotive waste heat recovery systems. Applied Energy 2013;105:293-303.

[3] David G., Michel F., Sanchez L., Waste heat recovery projects using organic Rankine cycle technology: Examples of biogas engines and steel mills applications. World Engineers Convention; 2011; Geneva.

[4] Sung T., Yun E., Kim H.D., Yoon S.Y., Choi B.S., Kim K., Kim J., Jung Y.B., Kim K.C., Performance characteristics of a 200-kw organic Rankine cycle system in a steel processing plant. Applied Energy 2016;183:623-635.
[5] Gurgenci H., Performance of power plants with organic Rankine cycles under part-load and off-design conditions. Solar Energy 1986;36(1):45-51.
[6] Sun J., Li W., Operation optimization of an organic Rankine cycle (orc) heat recovery power plant. Applied Thermal Engineering 2011;31(1112):2032-2041.
[7] Manente G., Toffolo A., Lazzaretto A., Paci M., An organic Rankine cycle off -design model for the search of the optimal control strategy. Energy 2013;58:97-106.
[8] Ibarra M., Rovira A., Alarco´n-Padilla D.C., Zaragoza G., Blanco J., Performance of a 5 kwe solar only organic Rankine unit coupled to a reverse osmosis plant. Energy Procedia (2014);49: 2251 –2260.
[9] Hu D., Zheng Y., Wu Y., Li S., Dai Y., Off-design performance comparison of an organic Rankine cycle under different control strategies, Applied Energy 2015;156:268 – 279.
[10] Lecompte S., Huisseune H., van den Broek M., Vanslambrouck B., De Paepe M., Review of organic Rankine cycle (orc) architectures for waste heat recovery, Renewable and Sustainable Energy Reviews 2015;47:448-461.
[11] Lecompte S., Huisseune H., van den Broek M., De Paepe M., Methodical thermodynamic analysis and regression models of organic Rankine cycle architectures for waste heat recovery. Energy 2015;87:60-76.
[12] Saleh B., Koglbauer G., Wendland M., Fischer J., Working fluids for low-temperature organic Rankine cycles. Energy 2007;32(7):1210-1221.
[13] Wang Z.Q., Zhou N.J, Guo J., Wang X.Y., Fluid selection and parametric optimization of organic Rankine cycle using low temperature waste heat. Energy 2012;40(1):107-115.
[14] Yamada N., Mohamad M.N., Kien T.T., Study on thermal efficiency of low- to medium temperature organic Rankine cycles using hfo-1234yf. Renewable Energy 2012;41:368-375.
[15] Liu B.T., Chien K.H., Wang C.C., Effect of working fluids on organic Rankine cycle for waste heat recovery. Energy 2004;29(8):1207-1217.
[16] Dai Y., Wang J., Gao L., Parametric optimization and comparative study of organic Rankine cycle (orc) for low grade waste heat recovery. Energy Conversion and Management 2009;50(3):576-582.
[17] Hung T.C., Wang S.K., Kuo C.H., Pei B.S., Tsai K.F., A study of organic working fluids on system efficiency of an ORC using low-grade energy sources. Energy 2010;35(3):1403-1411.
[18] Oyewunmi O.A., Taleb A.I., Haslam A.J., Markides C.N., On the use of saft-vr mie for assessing large glide fluorocarbon working-fluid mixtures in organic Rankine cycles. Applied Energy 2016;163:263-282.
[19] Ho T., Mao S.S., Greif R., Comparison of the organic flash cycle (OFC) to other advanced vapor cycles for intermediate and high temperature waste heat reclamation and solar thermal energy. Energy 2012;42(1):213-223.
[20] Pascale A.D., Ferrari C., Melino F., Morini M., Pinelli M., Integration between a thermophotovoltaic generator and an organic rankine cycle. Applied Energy 2012;97:695-703.
[21] Öhman H., Lundqvist P., Comparison and analysis of performance using low temperature power cycles. Applied Thermal Engineering 2013;52(1):160-169.
[22] Wieland C., Meinel D., Eyerer S., Spliethof H., Innovative CHP concept for ORC and its benefit compared to conventional concepts. Applied Energy 2016;183:478-490.
[23] Li C., Wang H., Power cycles for waste heat recovery from medium to high temperature flue gas sources from a view of thermodynamic optimization. Applied Energy 2016;180:707 – 721.
[24] Lecompte S., Performance evaluation of organic Rankine cycle architectures: application to waste heat valorisation [dissertation]. Ghent, Belgium: Ghent University; 2016.
[25] Qiao H., Aute V., Lee H., Saleh K., Radermacher R., A new model for plate heat exchangers with generalized flow configurations and phase change. International Journal of Refrigeration 2013;36(2):622-632.

[26] Cuevas C., Lebrun J., Lemort V., Ngendakumana P., Development and validation of a condenser three zones model, Applied Thermal Engineering 2009;29(1718):3542 – 3551.
[27] Shah R., Sekulic D., Fundamentals of Heat Exchanger Design, Wiley, 2003.
[28] Martin H., VDI Heat Atlas, 2010, Ch. B6: Pressure Drop and Heat Transfer in Plate Heat Exchangers.
[29] Han D.H., Lee K.J., Kim Y.H., The characteristics of condensation in brazed plate heat and exchangers with different chevron angles. Journal of the Korean Physical Society 2003;43:66-73.
[30] Han D.H., Lee K.J., Kim Y.H., Experiments on the characteristics of evaporation of r410a in brazed plate heat exchangers with different geometric configurations. Applied Thermal Engineering 2003;23(10):1209-1225.
[31] Declaye S., Quoilin S., Guillaume L., Lemort V., Experimental study on an open-drive scroll expander integrated into an orc (organic Rankine cycle) system with r245fa as working fluid. Energy 2013;55:173-183
[32] Lemort V., Quoilin S., Cuevas C., Lebrun J., Testing and modeling a scroll expander inte364 grated into an organic Rankine cycle, Applied Thermal Engineering 2009;29(1415):3094-3102.
[33] Öhman H., Lundqvist P., Experimental investigation of a lysholm turbine operating with superheated, saturated and 2-phase inlet conditions. Applied Thermal Engineering 2013;50(1):1211-1218.
[34] Smith I.K., Stocik N., Aldis C.A., Lysholm machines as two-phase expanders. International Compressor Engineering Conference, 1994, Purdue.
[35] Li M., Ma Y., Tian H., A rolling piston-type two-phase expander in the transcritical co2 cycle. HVAC&R Research 2009;15:729-741.
[36] Öhman H., Lundqvist P., Screw expanders in orc applications, review and a new perspective, in: 3rd International Seminar on ORC Power Systems, 2015, Brussels, Belgium.
[37] Dick E., Fundamentals of Turbomachines. 1st Edition, Springer Netherlands, 2015.
[38] Derakhshan S., Nourbakhsh A., Experimental study of characteristic curves of centrifugal pumps working as turbines in different specific speeds. Experimental Thermal and Fluid Science 2008;32(3):800-807.
[39] Ziviani D., Gusev S., Lecompte S., Groll E.A., Braun J.E., Horton W.T., van den Broek M., De Paepe M., Characterizing the performance of a single-screw expander in a small-scale organic Rankine cycle for waste heat recovery, Applied Energy 2016;181:155-170.
[40] Quoilin S., Van den Broek M., Declaye S., Dewallef P., Lemort V., Techno-economic survey of organic Rankine cycle (orc) systems. Renewable and Sustainable Energy Reviews 2013;22:168-186.